

A NOTE ON ENERGY CONTRACTION AND OPTIMAL CONVERGENCE OF ADAPTIVE ITERATIVE LINEARIZED FINITE ELEMENT METHODS

PASCAL HEID¹, DIRK PRAETORIUS², AND THOMAS P. WIHLE¹

ABSTRACT. In this note, we revisit a unified methodology for the iterative solution of nonlinear equations in Hilbert spaces. Our key observation is that the general approach from [HW20a, HW20b] satisfies an energy contraction property in the context of (abstract) strongly monotone problems. This property, in turn, is the crucial ingredient in the recent convergence analysis in [GHPS20]. In particular, we deduce that adaptive iterative linearized finite element methods (AILFEMs) lead to linear convergence with optimal algebraic rates with respect to the degrees of freedom as well as the total computational time.

1. INTRODUCTION

On a real Hilbert space X with inner product $(\cdot, \cdot)_X$ and induced norm $\|\cdot\|_X$, we consider a nonlinear operator $F : X \rightarrow X^*$, where X^* denotes the dual space of X . We aim to generate optimally converging (with respect to the number of degrees of freedom and the total computational time) finite element approximations of the following nonlinear operator equation:

$$F(u) = 0 \quad \text{in } X^*. \quad (1)$$

In weak form, this problem reads:

$$\text{Find } u \in X \text{ such that } \langle F(u), v \rangle = 0 \quad \forall v \in X; \quad (2)$$

here, $\langle \cdot, \cdot \rangle$ signifies the duality pairing on $X^* \times X$. For the purpose of this work, we suppose that F satisfies the following conditions:

(F1) *Lipschitz continuity*: There exists a constant $L_F > 0$ such that

$$|\langle F(u) - F(v), w \rangle| \leq L_F \|u - v\|_X \|w\|_X \quad \forall u, v, w \in X.$$

(F2) *Strong monotonicity*: There exists a constant $\nu > 0$ such that

$$\nu \|u - v\|_X^2 \leq \langle F(u) - F(v), u - v \rangle \quad \forall u, v \in X.$$

(F3) The operator F possesses a *potential*, i.e., there exists a Gâteaux differentiable (energy) functional $E : X \rightarrow \mathbb{R}$ such that $E' = F$.

Assuming (F1) and (F2), the main theorem of strongly monotone operators guarantees that (1) (or equivalently (2)) has a unique solution $u^* \in X$; see, e.g., [Neč86, §3.3] or [Zei90, Thm. 25.B].

⁽¹⁾ MATHEMATICS INSTITUTE, UNIVERSITY OF BERN, SIDLERSTR. 5, CH-3012 BERN, SWITZERLAND

⁽²⁾ TU WIEN, INSTITUTE OF ANALYSIS AND SCIENTIFIC COMPUTING, WIEDNER HAUPTSTR. 8–10/E101/4, 1040 WIEN, AUSTRIA

E-mail addresses: pascal.heid@math.unibe.ch, dirk.praetorius@asc.tuwien.ac.at, wihler@math.unibe.ch.

2010 *Mathematics Subject Classification*. 35J62, 41A25, 47J25, 47H05, 47H10, 49M15, 65J15, 65N12, 65N22, 65N30, 65N50, 65Y20.

Key words and phrases. Iterative linearized Galerkin methods, fixed point iterations, Lipschitz continuous and strongly monotone operators, second-order elliptic problems, energy contraction, adaptive mesh refinement, convergence of adaptive FEM, optimal computational cost.

The authors acknowledge the financial support of the Swiss National Science Foundation (SNF), Grant No. 200021_182524, and of the Austrian Science Fund (FWF) Grant No. SFB F65 and P33216.

1.1. Iterative linearization. Following the recent approach [HW20a], we apply a general fixed point iteration scheme for (1). For given $v \in X$, we consider a linear and invertible *preconditioning operator* $A[v] : X \rightarrow X^*$. Then, the nonlinear problem (1) is equivalent to $A[u]u = f(u) := A[u]u - F(u)$. For any suitable initial guess $u^0 \in X$, this leads to the following iterative scheme:

$$\text{Find } u^{n+1} \in X \text{ such that } A[u^n]u^{n+1} = f(u^n) \quad \text{in } X^* \quad \forall n \geq 0. \quad (3)$$

Note that the above iteration is a *linear equation* for u^{n+1} , thereby rendering (3) an *iterative linearization scheme* for (1). Given $u^n \in X$, the weak form of (3) is based on the bilinear form $a(u^n; v, w) := \langle A[u^n]v, w \rangle$, for $v, w \in X$, and the solution $u^{n+1} \in X$ of (3) can be obtained from

$$a(u^n; u^{n+1}, w) = \langle f(u^n), w \rangle \quad \forall w \in X. \quad (4)$$

Throughout, for any $u \in X$, we suppose that the bilinear form $a(u; \cdot, \cdot)$ is uniformly coercive and bounded, i.e., there are two constants $\alpha, \beta > 0$ independent of $u \in X$ such that

$$a(u; v, v) \geq \alpha \|v\|_X^2 \quad \forall v \in X, \quad (5)$$

and

$$a(u; v, w) \leq \beta \|v\|_X \|w\|_X \quad \forall v, w \in X. \quad (6)$$

For any given $u^n \in X$, owing to the Lax–Milgram theorem, these two properties imply that the linear equation (4) admits a unique solution $u^{n+1} \in X$.

1.2. Iterative linearized Galerkin approach (ILG). In order to cast (4) into a computational framework, we consider closed (and mainly finite dimensional) subspaces $Y \subseteq X$, endowed with the inner product and norm on X . Then, ILG [HW20a] is based on restricting the weak iteration scheme (4) to Y . Specifically, for a prescribed initial guess $u_Y^0 \in Y$, define a sequence $\{u_Y^n\}_{n \geq 0} \subset Y$ inductively by

$$a(u_Y^n; u_Y^{n+1}, w) = \langle f(u_Y^n), w \rangle \quad \forall w \in Y. \quad (7)$$

Note that (7) has a unique solution, since the conditions (5) and (6) above remain valid for the restriction to $Y \subseteq X$. For the purpose of the convergence results in this paper, we introduce a *monotonicity condition* on the functional E from (F3).

(F4) There exists a (uniform) constant $C_E > 0$ such that for any closed subspace $Y \subseteq X$, the sequence defined by (7) fulfils the bound

$$E(u_Y^n) - E(u_Y^{n+1}) \geq C_E \|u_Y^n - u_Y^{n+1}\|_X^2 \quad \forall n \geq 0, \quad (8)$$

where E is the potential of F (restricted to $Y \subseteq X$) introduced in (F3).

If F satisfies (F1)–(F3) and if the ILG bilinear form $a(\cdot; \cdot, \cdot)$ from (4) is coercive (5) with coercivity constant $\alpha > L_F/2$, then (F4) is fulfilled; see [HW20b, Prop. 2.1]. Moreover, upon imposing alternative conditions, we may still be able to satisfy (8) even when $\alpha \leq L_F/2$. For instance, [HW20a, Rem. 2.8] proposed an *a posteriori* step size strategy that guarantees the bound (8) in the context of the damped Newton method. This argument can be generalized to other methods containing a damping parameter. Moreover, the Kačanov linearization approach (see (22) below) satisfies (8) with $C_E = \alpha/2$ without requiring $\alpha > L_F/2$; see, e.g., [HW20a, Eq. (18)].

1.3. Adaptive iterative linearized finite element method (AILFEM). We restrict ILG (7) to a sequence of Galerkin subspaces $X_0 \subset X_1 \subset X_2 \subset \dots \subset X_N \subset \dots \subset X$ with corresponding sequences $\{u_N^n\}_{n \geq 0} \subset X_N$ for $N \geq 0$ given by

$$a(u_N^n; u_N^{n+1}, v) = \langle f(u_N^n), v \rangle \quad \forall v \in X_N. \quad (9)$$

The spaces X_N will be conforming finite element spaces associated to admissible triangulations \mathcal{T}_N of an underlying bounded Lipschitz domain $\Omega \subset \mathbb{R}^d$, with $d \geq 2$. AILFEM (Algorithm 1 below) exploits an interplay of adaptive mesh refinements and ILG (9) and chooses the initial guesses $u_0^0 \in X_0$ and $u_{N+1}^0 = u_N^{n(N)} \in X_N \subset X_{N+1}$ for all $N \geq 0$ and appropriate indices $n(N) \geq 1$.

1.4. Goal of the paper. The work [GHPS18] has recently analyzed the AILFEM for the solution of (1) in the specific context of a Zarantonello linearization approach originally proposed in [CW17]. The results of [GHPS18] have been extended to contractive iterative solvers in [GHPS20]. In particular, it has been shown that an optimal convergence rate with respect to the number of degrees of freedom as well as with respect to the overall computational cost can be achieved. The purpose of the present note is to show that these optimality results from [GHPS20] also apply to AILFEM beyond the Zarantonello linearization approach (cf. [HW20b] for some convergence results in abstract spaces). Especially, we will exploit (F4) to establish an energy contraction property for the fixed point iteration (3), which constitutes the crucial ingredient in the analysis of [GHPS20]. In particular, we will revisit a few example AILFEM schemes from [HW20a], and verify our theoretical findings numerically.

2. ENERGY CONTRACTION

In this section, we will establish an energy contraction result for ILG (7). To this end, let $Y \subseteq X$ be a closed linear subspace of X as in §1.2. Moreover, denote by $u_Y^* \in Y$ the unique solution of the equation

$$\langle F(u_Y^*), v \rangle = 0 \quad \forall v \in Y, \quad (10)$$

where existence and uniqueness of u_Y^* follows again from the main theorem of strongly monotone operators.

Proposition 2.1. *Consider the sequence $\{u_Y^n\}_{n \geq 0} \subset Y$ generated by the iteration (7). If (F1)–(F4) are satisfied and $a(u; \cdot, \cdot)$ fulfils (5)–(6) for any $u \in Y$, then there holds the energy contraction property*

$$0 \leq E(u_Y^{n+1}) - E(u_Y^*) \leq q_{12}^2 [E(u_Y^n) - E(u_Y^*)] \quad \forall n \geq 0, \quad (11)$$

with a contraction constant

$$0 \leq q_{12} := (1 - 2C_E \nu^2 \beta^{-2} L_F^{-1})^{1/2} < 1 \quad (12)$$

independent of the subspace Y and of the iteration number n . In addition, the sequence $\{u_Y^n\}_{n \geq 0}$ converges to the unique solution $u_Y^* \in Y$ of (10).

Proof. With (F2) and since u_Y^* is the (unique) solution of (10), for $n \geq 0$, we first observe that

$$\nu \|u_Y^* - u_Y^n\|_X^2 \stackrel{(F2)}{\leq} \langle F(u_Y^*) - F(u_Y^n), u_Y^* - u_Y^n \rangle \stackrel{(10)}{=} \langle F(u_Y^n), u_Y^n - u_Y^* \rangle.$$

Recalling that $f(u) = A[u]u - F(u)$, (7) and (6) prove that

$$\langle F(u_Y^n), u_Y^n - u_Y^* \rangle \stackrel{(7)}{=} a(u_Y^n; u_Y^n - u_Y^{n+1}, u_Y^n - u_Y^*) \stackrel{(6)}{\leq} \beta \|u_Y^{n+1} - u_Y^n\|_X \|u_Y^n - u_Y^*\|_X.$$

Altogether, we derive the *a posteriori* error estimate

$$\|u_Y^* - u_Y^n\|_X \leq \beta \nu^{-1} \|u_Y^n - u_Y^{n+1}\|_X \quad \forall n \geq 0. \quad (13)$$

Next, we exploit the structural assumptions (F1)–(F3) to obtain the well-known inequalities

$$\frac{\nu}{2} \|u_Y^* - v\|_X^2 \leq E(v) - E(u_Y^*) \leq \frac{L_F}{2} \|u_Y^* - v\|_X^2 \quad \forall v \in Y; \quad (14)$$

see, e.g., [HW20b, Lem. 2.3] or [GHPS18, Lem. 5.1]. For any $n \geq 0$, we thus infer that

$$\begin{aligned} 0 &\stackrel{(14)}{\leq} E(u_Y^{n+1}) - E(u_Y^*) = E(u_Y^n) - E(u_Y^*) - [E(u_Y^n) - E(u_Y^{n+1})] \\ &\stackrel{(8)}{\leq} E(u_Y^n) - E(u_Y^*) - C_E \|u_Y^n - u_Y^{n+1}\|_X^2 \\ &\stackrel{(13)}{\leq} E(u_Y^n) - E(u_Y^*) - \frac{C_E \nu^2}{\beta^2} \|u_Y^* - u_Y^n\|_X^2 \\ &\stackrel{(14)}{\leq} E(u_Y^n) - E(u_Y^*) - \frac{2C_E \nu^2}{\beta^2 L_F} [E(u_Y^n) - E(u_Y^*)] = q_{12}^2 [E(u_Y^n) - E(u_Y^*)]. \end{aligned}$$

This proves, in particular, that $0 \leq q_{12}^2 < 1$. Finally, iterating this inequality, we obtain that

$$0 \leq \frac{\nu}{2} \|u_Y^* - u_Y^n\|_X^2 \stackrel{(14)}{\leq} \mathbf{E}(u_Y^n) - \mathbf{E}(u_Y^*) \leq q_{12}^{2n} [\mathbf{E}(u_Y^0) - \mathbf{E}(u_Y^*)] \quad \forall n \geq 0.$$

In particular, we conclude that $u_Y^n \rightarrow u_Y^*$ in Y as $n \rightarrow \infty$. \square

3. ADAPTIVE FINITE ELEMENT DISCRETIZATION

In this section, we thoroughly formulate AILFEM. For each $N \geq 0$, the space X_N in (9) will be a conforming finite element space that is associated to an admissible triangulation \mathcal{T}_N of an underlying bounded Lipschitz domain $\Omega \subset \mathbb{R}^d$, with $d \geq 2$. Following the recent approach [GHPS20], we will present an adaptive iterative linearization finite element algorithm that exploits the interplay of adaptive mesh refinements and the iterative scheme (9). Throughout this section, we will always assume that F satisfies (F1)–(F4) and that (5) and (6) hold true.

3.1. Mesh refinements. We adopt the framework from [GHPS20, §2.2–2.4], with slightly modified notation. Consider a shape-regular mesh refinement strategy $\mathbf{refine}(\cdot)$ such as, e.g., newest vertex bisection [Mit91]. For a subset \mathcal{M}_N of marked elements in a regular triangulation \mathcal{T}_N , let $\mathbf{refine}(\mathcal{T}_N, \mathcal{M}_N)$ be the coarsest regular refinement of \mathcal{T}_N such that all elements \mathcal{M}_N have been refined. Specifically, we write $\mathbf{refine}(\mathcal{T}_N)$ for the set of all possible meshes that can be generated from \mathcal{T}_N by (repeated) use of $\mathbf{refine}(\cdot)$. For a mesh $\mathcal{T}_N^{\text{ref}} \in \mathbf{refine}(\mathcal{T}_N)$, we assume the nestedness of the corresponding finite element spaces X_N^{ref} and X_N , respectively, i.e., $X_N \subseteq X_N^{\text{ref}}$. In the sequel, starting from a given initial triangulation \mathcal{T}_0 of Ω , we let $\mathbb{T} := \mathbf{refine}(\mathcal{T}_0)$ be the set of all possible refinements of \mathcal{T}_0 .

With regards to the optimal convergence rate of the algorithm with respect to the overall computational cost (see the next section §4), a few assumptions on the mesh refinement strategy are required, cf. [GHPS20, §2.8]. These are satisfied, in particular, for newest vertex bisection.

(R1) *Splitting property:* Each refined element is split into at least two and at most C_{ref} many subelements, where $C_{\text{ref}} \geq 2$ is a generic constant. In particular, for all triangulations $\mathcal{T} \in \mathbb{T}$, and for any $\mathcal{M} \subseteq \mathcal{T}$, the (one-level) refinement $\mathcal{T}' := \mathbf{refine}(\mathcal{T}, \mathcal{M})$ satisfies

$$\#(\mathcal{T} \setminus \mathcal{T}') + \#\mathcal{T} \leq \#\mathcal{T}' \leq C_{\text{ref}} \#(\mathcal{T} \setminus \mathcal{T}') + \#(\mathcal{T} \cap \mathcal{T}').$$

Here, $\mathcal{T} \setminus \mathcal{T}'$ is the set of all elements in \mathcal{T} which have been refined in \mathcal{T}' , and $\mathcal{T} \cap \mathcal{T}'$ comprises all unrefined elements.

(R2) *Overlay estimate:* For all meshes $\mathcal{T} \in \mathbb{T}$, and refinements $\mathcal{T}_1^{\text{ref}}, \mathcal{T}_2^{\text{ref}} \in \mathbf{refine}(\mathcal{T})$ there exists a common refinement denoted by

$$\mathcal{T}_1^{\text{ref}} \oplus \mathcal{T}_2^{\text{ref}} \in \mathbf{refine}(\mathcal{T}_1^{\text{ref}}) \cap \mathbf{refine}(\mathcal{T}_2^{\text{ref}}) \subseteq \mathbf{refine}(\mathcal{T}),$$

which satisfies $\#(\mathcal{T}_1^{\text{ref}} \oplus \mathcal{T}_2^{\text{ref}}) \leq \#\mathcal{T}_1^{\text{ref}} + \#\mathcal{T}_2^{\text{ref}} - \#\mathcal{T}$.

(R3) *Mesh-closure estimate:* There exists a constant $C_{\text{mesh}} > 0$ such that, for each sequence $\{\mathcal{T}_N\}_{N \geq 1}$ of successively refined meshes, i.e., $\mathcal{T}_{N+1} := \mathbf{refine}(\mathcal{T}_N, \mathcal{M}_N)$ for some $\mathcal{M}_N \subseteq \mathcal{T}_N$, it holds that

$$\#\mathcal{T}_N - \#\mathcal{T}_0 \leq C_{\text{mesh}} \sum_{J=0}^{N-1} \#\mathcal{M}_J \quad \forall N \in \mathbb{N}.$$

3.2. Error estimators. For a mesh $\mathcal{T}_N \in \mathbb{T}$ associated to a discrete space X_N , suppose that there exists a *computable local refinement indicator* $\eta_N : \mathcal{T}_N \times X_N \rightarrow \mathbb{R}$, with $\eta_N(T, v) \geq 0$ for all $T \in \mathcal{T}_N$ and $v \in X_N$. Then, for any $v \in X_N$ and $\mathcal{U}_N \subseteq \mathcal{T}_N$, let

$$\eta_N(\mathcal{U}_N, v) := \left(\sum_{T \in \mathcal{U}_N} \eta_N(T, v)^2 \right)^{1/2} \quad \text{and} \quad \eta_N(v) := \eta_N(\mathcal{T}_N, v). \quad (15)$$

We recall the following axioms of adaptivity from [CFPP14] for the refinement indicators: There are fixed constants C_{stb} , $C_{\text{rel}} \geq 1$ and $0 < q_{\text{red}} < 1$ such that, for all $\mathcal{T}_N \in \mathbb{T}$ and $\mathcal{T}_N^{\text{ref}} \in \mathbf{refine}(\mathcal{T}_N)$, with associated refinement indicators η_N and η_N^{ref} , the following properties hold, cf. [GHPS20, §2.8]:

- (A1) *Stability*: $|\eta_N(\mathcal{U}_N, v) - \eta_N^{\text{ref}}(\mathcal{U}_N, w)| \leq C_{\text{stb}} \|v - w\|_X$, for all $v \in X_N, w \in X_N^{\text{ref}}$ and all $\mathcal{U}_N \subseteq \mathcal{T}_N \cap \mathcal{T}_N^{\text{ref}}$.
- (A2) *Reduction*: $\eta_N^{\text{ref}}(\mathcal{T}_N^{\text{ref}} \setminus \mathcal{T}_N, v) \leq q_{\text{red}} \eta_N(\mathcal{T}_N \setminus \mathcal{T}_N^{\text{ref}}, v)$, for all $v \in X_N$.
- (A3) *Reliability*: For the error between the exact solution $u^* \in X$ of (1) and the exact discrete solution $u_N^* \in X_N$ of (10), we have the *a posteriori* error estimate $\|u^* - u_N^*\|_X \leq C_{\text{rel}} \eta_N(u_N^*)$.
- (A4) *Discrete reliability*: $\|u_N^{*,\text{ref}} - u_N^*\|_X \leq C_{\text{rel}} \eta_N(\mathcal{T}_N \setminus \mathcal{T}_N^{\text{ref}}, u_N^*)$, where $u_N^{*,\text{ref}} \in X_N^{\text{ref}}$ is the solution of (10) on the discrete space X_N^{ref} associated with $\mathcal{T}_N^{\text{ref}}$.

We emphasize that (A1)–(A4) are satisfied for the usual h -weighted residual error estimators in the specific context of our application in section §5, cf. (23).

3.3. AILFEM algorithm. We recall the adaptive algorithm from [GHPS18] (and its generalization [GHPS20]), which was studied in the specific context of finite element discretizations of the Zarantonello iteration. These algorithms are closely related to the general adaptive ILG approach in [HW20a]. The key idea is the same in all algorithms: On a given discrete space, we iterate the linearization scheme (9) as long as the linearization error estimator dominates. Once the ratio of the linearization error estimator $[\mathbb{E}(u_N^n) - \mathbb{E}(u_N^{n-1})]^{1/2}$ and the *a posteriori* error estimator $\eta_N(u_N^n)$ falls below a prescribed tolerance, the discrete space is refined appropriately.

Algorithm 1 AILFEM algorithm

- 1: Prescribe adaptivity parameters $\lambda > 0$, $0 < \theta \leq 1$, and $C_{\text{mark}} \geq 1$. Moreover, set $N := 0$ and $n := 0$. Start with an initial triangulation \mathcal{T}_0 , a corresponding finite element space X_0 , and an arbitrary initial guess $u_0^0 \in X_0$.
 - 2: **while** true **do**
 - 3: **repeat** with $n \leftarrow 0$
 - 4: Perform a single iterative linearization step (9) on X_N to obtain u_N^{n+1} from u_N^n .
 - 5: Update $n \leftarrow n + 1$.
 - 6: **until** $[\mathbb{E}(u_N^n) - \mathbb{E}(u_N^{n-1})]^{1/2} \leq \lambda \eta_N(u_N^n)$
 - 7: Determine a marking set $\mathcal{M}_N \subseteq \mathcal{T}_N$ with minimal cardinality (up to the multiplicative constant $C_{\text{mark}} \geq 1$) such that $\theta \eta_N(u_N^n) \leq \eta_N(\mathcal{M}_N, u_N^n)$, and set $\mathcal{T}_{N+1} := \text{refine}(\mathcal{T}_N, \mathcal{M}_N)$.
 - 8: Set $\mathfrak{n}(N) := n$ and define $u_{N+1}^0 := u_N^{\mathfrak{n}(N)}$ by inclusion $X_{N+1} \supseteq X_N$.
 - 9: Update $N \leftarrow N + 1$.
 - 10: **end while.**
-

Remark 3.1. Under the conditions (A1) and (A3), we notice some facts about Algorithm 1 from [GHPS20, Prop. 3] and [GHPS18, Prop. 4.5 & 4.6]: For any $N \geq 0$, there holds the *a posteriori* error estimate

$$\|u^* - u_N^{\mathfrak{n}(N)}\|_X \leq C_{16} \eta_N(u_N^{\mathfrak{n}(N)}), \quad (16)$$

where C_{16} depends only on $\nu, \beta, \lambda, L_F, C_{\text{rel}}, C_{\text{stb}}$, and C_E . In particular, if the repeat loop terminates with $\eta_N(u_N^{\mathfrak{n}(N)}) = 0$ for some $N \geq 0$, then $u_N^{\mathfrak{n}(N)} = u^*$, i.e., the exact solution is obtained. Moreover, in the non-generic case that the repeat loop in Algorithm 1 does not terminate after finitely many steps, for some $N \geq 0$, the generated sequence $\{u_N^n\}_{n \geq 0}$ converges to $u_N^* = u^*$ (in particular, the solution u^* is discrete).

4. OPTIMAL CONVERGENCE

We are now ready to outline the linear convergence of the sequence of approximations from Algorithm 1 to the unique solution of (1). In addition, the rate optimality with respect to the overall computational costs will be discussed.

4.1. Step counting. Following [GHPS20], we introduce an ordered index set

$$\mathcal{Q} := \{(N, n) \in \mathbb{N}_0^2 : \text{index pair } (N, n) \text{ occurs in Algorithm 1} \wedge n < \mathbf{n}(N)\},$$

where $\mathbf{n}(N) \geq 1$ counts the number of steps in the repeat loop for each N . We exclude the pair $(N, \mathbf{n}(N))$ from \mathcal{Q} , since either $u_{N+1}^0 = u_N^{\mathbf{n}(N)}$ and $(N+1, 0) \in \mathcal{Q}$ or even $\mathbf{n}(N) := \infty$ if the loop does not terminate after finitely many steps; see also Remark 3.1. Observing that Algorithm 1 is sequential, the index set \mathcal{Q} is naturally ordered: For $(N, n), (N', n') \in \mathcal{Q}$, we write $(N', n') < (N, n)$ if and only if (N', n') appears earlier in Algorithm 1 than (N, n) . With this order, we can define the *total step counter*

$$|(N, n)| := \#\{(N', n') \in \mathcal{Q} : (N', n') < (N, n)\} = n + \sum_{N'=0}^{N-1} \mathbf{n}(N'),$$

which provides the total number of solver steps up to the computation of u_N^n . Finally, we introduce the notation $\mathfrak{N} := \sup\{N \in \mathbb{N} : (N, 0) \in \mathcal{Q}\}$.

4.2. Linear convergence. Based on the notation used in Algorithm 1, let us introduce the quasi-error

$$\Delta_N^n := \|u^* - u_N^n\|_X + \eta_N(u_N^n) \quad \forall (N, n) \in \overline{\mathcal{Q}} := \mathcal{Q} \cup \{(N, \mathbf{n}(N)) : \mathbf{n}(N) < \infty\}, \quad (17)$$

and suppose that the estimator η_N satisfies (A1)–(A3). Then, appealing to the energy contraction property from Proposition 2.1, we make the crucial observation that ILG (7) satisfies the contraction property (C1) from [GHPS20]. Consequently, [GHPS20, Thm. 4] directly applies to our setting:

Theorem 4.1 ([GHPS20, Thm. 4]). *Suppose (A1)–(A3). Then, for all $0 < \theta \leq 1$ and $0 < \lambda < \infty$, there exist constants $C_{\text{lin}} \geq 1$ and $0 < q_{\text{lin}} < 1$ such that the quasi-error (17) is linearly convergent in the sense of*

$$\Delta_N^n \leq C_{\text{lin}} q_{\text{lin}}^{|(N,n)| - |(N',n')|} \Delta_{N'}^{n'} \quad \forall (N, n), (N', n') \in \mathcal{Q} \text{ with } (N', n') < (N, n).$$

The constants C_{lin} and q_{lin} depend only on $L_F, \nu, \beta, C_E, C_{\text{stb}}, q_{\text{red}}, C_{\text{rel}}$, and the adaptivity parameters θ and λ .

4.3. Optimal convergence rate and computational work. Furthermore, we address the optimal convergence rate of the quasi-error (17) with respect to the degrees of freedom as well as the computational work. As before, we can directly apply a result from [GHPS20] owing to the energy contraction from Proposition 2.1. For its statement, we need further notation: First, for $L \in \mathbb{N}_0$, let $\mathbb{T}(L)$ be the set of all refinements \mathcal{T} of \mathcal{T}_0 with $\#\mathcal{T} - \#\mathcal{T}_0 \leq L$. Next, for $s > 0$, define

$$\|u^*\|_{\mathbb{A}_s} := \sup_{L \in \mathbb{N}} (L+1)^s \inf_{\mathcal{T}_{\text{opt}} \in \mathbb{T}(L)} [\|u^* - u_{\text{opt}}^*\|_X + \eta_{\text{opt}}(u_{\text{opt}}^*)] \in \mathbb{R}_{\geq 0} \cup \{\infty\},$$

where u_{opt}^* is the discrete solution (10) on the finite element space related to an *optimal* (in terms of the above infimum) mesh \mathcal{T}_{opt} . For $s > 0$, we note that $\|u^*\|_{\mathbb{A}_s} < \infty$ if and only if the quasi-error converges at least with rate s along a sequence of optimal meshes.

Theorem 4.2 ([GHPS20, Thm. 7]). *Suppose (R1)–(R3) and (A1)–(A4), and define*

$$\lambda_{\text{opt}} := \frac{1 - q_{12}}{q_{12} C_{\text{stb}}} \sqrt{\nu/2}.$$

Let $0 < \theta \leq 1$ and $0 < \lambda < \lambda_{\text{opt}} \theta$ such that

$$0 < \theta' := \frac{\theta + \lambda/\lambda_{\text{opt}}}{1 - \lambda/\lambda_{\text{opt}}} < (1 + C_{\text{stb}}^2 C_{\text{rel}}^2)^{-1/2}.$$

Then, for any $s > 0$, there exist positive constants $c_{\text{opt}}, C_{\text{opt}}$ such that

$$\begin{aligned} c_{\text{opt}}^{-1} \|u^*\|_{\mathbb{A}_s} &\leq \sup_{(N', n') \in \mathcal{Q}} (\#\mathcal{T}_{N'} - \#\mathcal{T}_0 + 1)^s \Delta_{N'}^{n'} \\ &\leq \sup_{(N', n') \in \mathcal{Q}} \left(\sum_{\substack{(N, n) \in \mathcal{Q} \\ (N, n) \leq (N', n')}} \#\mathcal{T}_N \right)^s \Delta_{N'}^{n'} \leq C_{\text{opt}} \max\{\|u^*\|_{\mathbb{A}_s}, \Delta_0^0\}. \end{aligned} \quad (18)$$

Here, the constant $c_{\text{opt}} > 0$ depends only on $\nu, L_F, C_{\text{ref}}, C_{\text{stb}}, C_{\text{rel}}, \#\mathcal{T}_0$, and s , and additionally on \mathfrak{N} and N_0 , respectively, if $\mathfrak{N} < \infty$ or $\eta_{N_0}(u_{N_0}^{n(N_0)}) = 0$ for some $(N_0 + 1, 0) \in \mathcal{Q}$, respectively; moreover, the constant $C_{\text{opt}} > 0$ depends only on $C_{16}, \nu, C_{\text{stb}}, q_{\text{red}}, C_{\text{rel}}, C_{\text{mesh}}, 1 - \lambda/\lambda_{\text{opt}}, C_{\text{mark}}, C_{\text{lin}}, q_{\text{lin}}, \#\mathcal{T}_0$, and s .

The significance of (18) is that the quasi-error Δ_N^n from (17) decays at rate s (with respect to the number of elements or, equivalently, the number of degrees of freedom) if and only if rate s is achievable for the discrete solutions on optimal meshes (with respect to the number of elements). If, in addition, all of the (single) steps in Algorithm 1 can be performed at linear cost, $\mathcal{O}(\#\mathcal{T}_N)$, then the quasi-error even decays with rate s with respect to the overall computational cost if and only if rate s is attainable with respect to the number of elements. We note that the total computational cost is proportional to the total computational time, which is therefore monitored in the subsequent numerical experiment.

5. NUMERICAL EXPERIMENT

In this section, we test Algorithm 1 with a numerical example.

5.1. Model problem. On an open, bounded, and polygonal domain $\Omega \subset \mathbb{R}^2$ with Lipschitz boundary $\Gamma = \partial\Omega$, we consider the quasi-linear second-order elliptic boundary value problem:

$$\text{Find } u \in X \text{ such that } \mathbf{F}(u) := -\nabla \cdot \{\mu(|\nabla u|^2) \nabla u\} - g = 0 \quad \text{in } X^*. \quad (19)$$

Here, $X := H_0^1(\Omega)$ is the standard Sobolev space of H^1 -functions on Ω with zero trace along Γ . For $u, v \in X$, the inner product and norm on X are defined by $(u, v)_X := (\nabla u, \nabla v)_{L^2(\Omega)}$ and $\|u\|_X := \|\nabla u\|_{L^2(\Omega)}$, respectively. We suppose that $g \in X^* = H^{-1}(\Omega)$ in (19) is given, and the diffusion parameter $\mu \in C^1([0, \infty))$ fulfils the monotonicity property

$$m_\mu(t - s) \leq \mu(t^2)t - \mu(s^2)s \leq M_\mu(t - s) \quad \forall t \geq s \geq 0, \quad (20)$$

with constants $M_\mu \geq m_\mu > 0$. Under this condition, the nonlinear operator $\mathbf{F} : H_0^1(\Omega) \rightarrow H^{-1}(\Omega)$ from (19) satisfies (F1) and (F2) with $\nu = m_\mu$ and $L_F = 3M_\mu$; see [Zei90, Prop. 25.26]. Moreover, \mathbf{F} has a potential $\mathbf{E} : X \rightarrow \mathbb{R}$ given by

$$\mathbf{E}(u) := \int_{\Omega} \psi(|\nabla u|^2) \, d\mathbf{x} - \langle g, u \rangle \quad \forall u \in X,$$

where $\psi(s) := 1/2 \int_0^s \mu(t) \, dt$, $s \geq 0$. The weak form of the boundary value problem (19) reads:

$$\text{Find } u \in X \text{ such that } \int_{\Omega} \mu(|\nabla u|^2) \nabla u \cdot \nabla v \, d\mathbf{x} = \langle g, v \rangle \quad \forall v \in X. \quad (21)$$

For the nonlinear boundary value problem (19), [HW20a, §5.1] proves the convergence of a few particular iterative linearization schemes, which can be cast into the general approach (4). These include the following:

(i) *Zarantonello (or Picard) iteration*, for $\delta_Z \in (0, 2/3M_\mu)$:

$$-\Delta u^{n+1} = -\Delta u^n - \delta_Z \mathbf{F}(u^n), \quad n \geq 0;$$

cf. Zarantonello's original report [Zar60] or the monographs [Neč86, §3.3] and [Zei90, §25.4]. We further point to [HW20b, Rem. 1] for the extended domain of the damping parameter δ_Z .

(ii) *Kačanov iteration*:

$$-\nabla \cdot \{\mu(|\nabla u^n|^2)\nabla u^{n+1}\} - g = 0, \quad n \geq 0; \quad (22)$$

cf. [Zei90, §25.13].

(iii) *Newton iteration*, for a damping parameter $0 < \delta_{\min} \leq \delta(u^n) \leq \delta_{\max} < 2m_\mu/3M_\mu$:

$$F'(u^n)u^{n+1} = F'(u^n)u^n - \delta(u^n)F(u^n), \quad n \geq 0;$$

Here, for $u \in X$, the Gâteaux derivative of F is given through

$$\langle F'(u)v, w \rangle = \int_{\Omega} 2\mu'(|\nabla u|^2)(\nabla u \cdot \nabla v)(\nabla u \cdot \nabla w) \, dx + \int_{\Omega} \mu(|\nabla u|^2)\nabla v \cdot \nabla w \, dx, \quad v, w \in X.$$

5.2. Discretization and local refinement indicator. AILFEM for (21) is based on regular triangulations $\{\mathcal{T}_N\}_{N \geq 0}$ that partition the domain Ω into open and disjoint triangles $T \in \mathcal{T}_N$ such that $\bar{\Omega} = \bigcup_{T \in \mathcal{T}_N} \bar{T}$. Moreover, we consider associated finite element spaces $X_N := \{v \in H_0^1(\Omega) : v|_T \in \mathcal{P}_1(T) \, \forall T \in \mathcal{T}_N\}$, where we signify by $\mathcal{P}_1(T)$ the space of all affine functions on $T \in \mathcal{T}_N$. The mesh refinement strategy `refine`(\cdot) in Algorithm 1 is given by newest vertex bisection [Mit91]. Moreover, for any $v \in X_N$ and any $T \in \mathcal{T}_N$, we define the local refinement indicator respectively the global error indicator from (15) by

$$\begin{aligned} \eta_N(T, v)^2 &:= h_T^2 \|g\|_{L^2(T)}^2 + h_T \left\| \llbracket \mu(|\nabla v|^2)\nabla v \rrbracket \right\|_{L^2(\partial T \setminus \Gamma)}^2, \\ \eta_N(v) &:= \left(\sum_{T \in \mathcal{T}_N} \eta_N(T, v)^2 \right)^{1/2}, \end{aligned} \quad (23)$$

where $\llbracket \cdot \rrbracket$ signifies the normal jump across element faces, and $h_T := |T|^{1/2}$ is equivalent to the diameter of $T \in \mathcal{T}$. This error estimator satisfies the assumptions (A1)–(A4) for the problem under consideration; see, e.g., [GMZ12, §3.2] or [CFPP14, §10.1].

5.3. Computational example. Consider the L-shaped domain $\Omega = (-1, 1)^2 \setminus ([0, 1] \times [-1, 0])$, and the nonlinear diffusion parameter $\mu(t) = 1 + e^{-t}$, which satisfies (20) with $m_\mu = 1 - 2 \exp(-3/2)$ and $M_\mu = 2$. Moreover, we choose g such that the analytical solution of (19) is given by

$$u^*(r, \varphi) = r^{2/3} \sin(2\varphi/3) (1 - r \cos \varphi)(1 + r \cos \varphi)(1 - r \sin \varphi)(1 + r \sin \varphi) \cos \varphi,$$

where r and φ are polar coordinates; this is the prototype singularity for (linear) second-order elliptic problems with homogeneous Dirichlet boundary conditions in the L-shaped domain; in particular, we note that the gradient of u^* is unbounded at the origin.

In all our experiments below we set the adaptive mesh refinement parameters to $\theta = 0.5$, and $C_{\text{mark}} = 1$. The computations employ an initial mesh \mathcal{T}_0 consisting of 192 uniform triangles, and with the starting guess $u_0^0 \equiv 0$. Then, the procedure is run until the number of elements exceeds 10^6 . We always choose the damping parameter $\delta = 1$ for the Newton iteration, and vary the damping parameter δ_Z for the Zarantonello iteration, as well as the adaptivity parameter λ , cf. line 6 in Algorithm 1, throughout the experiments. Our implementation is based on the MATLAB package [FPW11] with the necessary modifications.

In general, for the Newton scheme, we note that choosing the damping parameter to be $\delta = 1$ (potentially resulting in quadratic convergence of the iterative linearization close to the solution) might lead to a divergent iteration for the given boundary value problem (cf. [AW14]). Our numerical computations illustrate, however, that this is not of concern in the current experiments. Indeed, for $\delta = 1$, the bound (8) from (F4) remains satisfied in each iteration. Otherwise, a prediction and correction strategy which obeys the bound (8), could be employed (see [HW20a, Rem. 2.8]). This would guarantee the convergence of the (damped) Newton method.

(1) $\delta_Z = 0.1$ and $\lambda = 0.5$: In Figure 1, we display the performance of Algorithm 1 with respect to both the number of elements and the total computational time. We clearly see a convergence rate of $-1/2$ for the Kačanov and Newton method, which is optimal for linear finite elements. Moreover, the Zarantonello iteration has a pre-asymptotic phase of reduced convergence, which

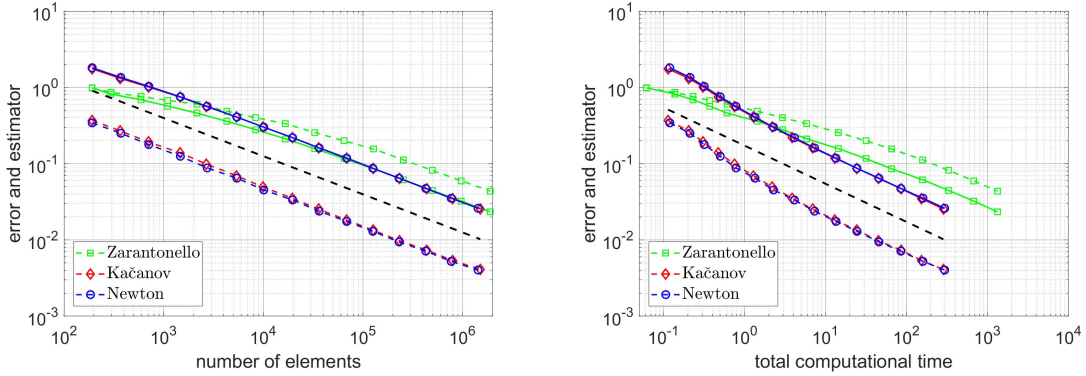


FIGURE 1. $\delta_Z = 0.1$ and $\lambda = 0.5$: Performance plot for adaptively refined meshes with respect to the number of elements (left) and the total computational time (right). The solid and dashed lines correspond to the estimator and the error, respectively. The dashed lines without any markers indicate the optimal convergence order of $-1/2$ for linear finite elements.

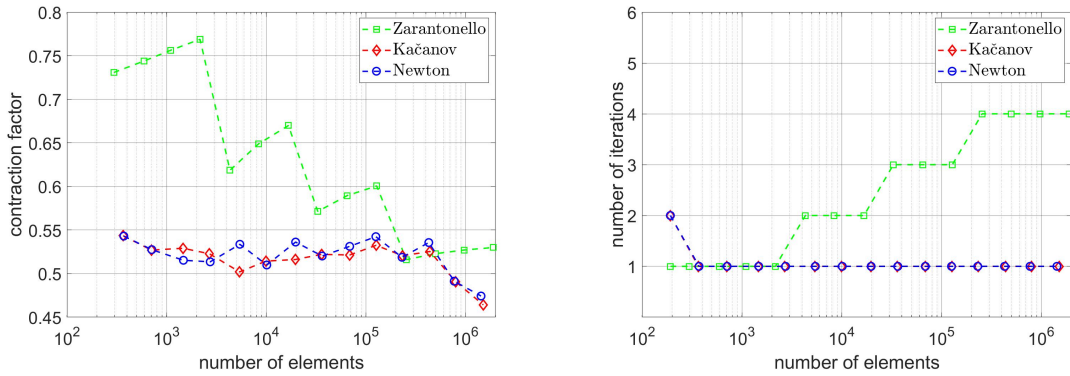


FIGURE 2. $\delta_Z = 0.1$ and $\lambda = 0.5$: The contraction factor \varkappa_N (left, see (24)) and the number of iterations (right) on each finite element space.

becomes optimal for finer meshes. In Figure 2 (left) we observe that the energy contraction factor given by

$$\varkappa_N := \frac{\mathbf{E}(u_N^{n(N)}) - \mathbf{E}(u^*)}{\mathbf{E}(u_N^0) - \mathbf{E}(u^*)} \quad (24)$$

is inferior for the Zarantonello iteration in the initial phase (compared to the Kačanov and Newton methods), which might explain the reduced convergence. This contraction factor becomes better for an increased number of iterations, see Figure 2 (right), thereby leading to the asymptotically optimal convergence rate for the Zarantonello iteration. Finally, in Figure 3 (left), we display the quotient

$$\kappa_N := \frac{\mathbf{E}(u_N^{n(N)-1}) - \mathbf{E}(u_N^{n(N)})}{\|u_N^{n(N)} - u_N^{n(N)-1}\|_X^2}, \quad (25)$$

which experimentally verifies the assumption (F4).

- (2) $\delta_Z = 0.3$ and $\lambda = 0.1$: As before, in Figure 4, we display the performance of Algorithm 1 with respect to both the number of elements and the total computational time. We clearly observe the optimal convergence rate of $-1/2$ for all of the three iteration schemes presented above

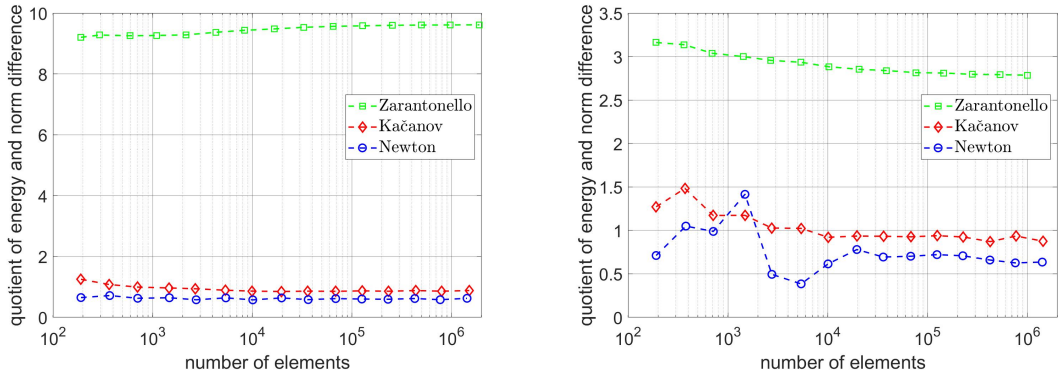


FIGURE 3. The quotient κ_N from (25) on each finite element space for $\delta_Z = 0.1$ and $\lambda = 0.5$ (left) and $\delta_Z = 0.3$ and $\lambda = 0.1$ (right), respectively.

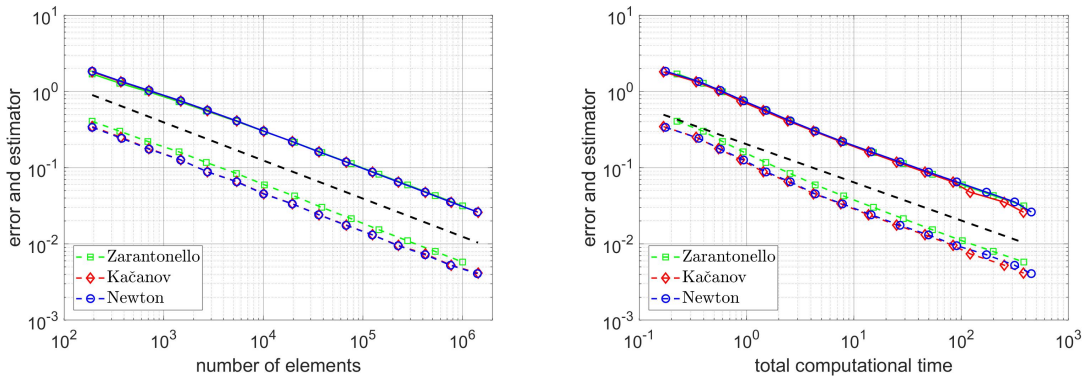


FIGURE 4. $\delta_Z = 0.3$ and $\lambda = 0.1$: Performance plot for adaptively refined meshes with respect to the number of elements (left) and the total computational time (right). The solid and dashed lines correspond to the estimator and the error, respectively. The dashed lines without any markers indicate the optimal convergence order of $-1/2$ for linear finite elements.

from the initial mesh onwards. In contrast to the experiment before, the energy contraction factor \varkappa_N from (24) is now of comparable size for all the iteration schemes, as we can see from Figure 5 (left). Moreover, the number of iterations does not significantly differ for the three iterative methods. Again, we plot in Figure 3 (right) the quotient (25) for the numerical evidence of the assumption (F4).

- (3) $\delta_Z = 0.3$ and $\lambda = 0.01$: Once more, we observe optimal convergence rate for all our three iteration schemes with respect to both the number of elements and the total computational time, see Figure 6. The total computational times obtained, however, differ noticeably, see Figure 6 (right), as a consequence of the varying number of iterative linearization steps of the three methods, see Figure 7 (right). In contrast, the energy contraction factor \varkappa_N from (24) almost coincides for the different iteration schemes, see Figure 7 (left), which is due to the small adaptivity parameter $\lambda = 0.01$.

6. CONCLUSIONS

We have established an energy contraction property for the iterative linearization Galerkin method (ILG, see (7)). This result is the decisive prerequisite to apply the convergence theorems

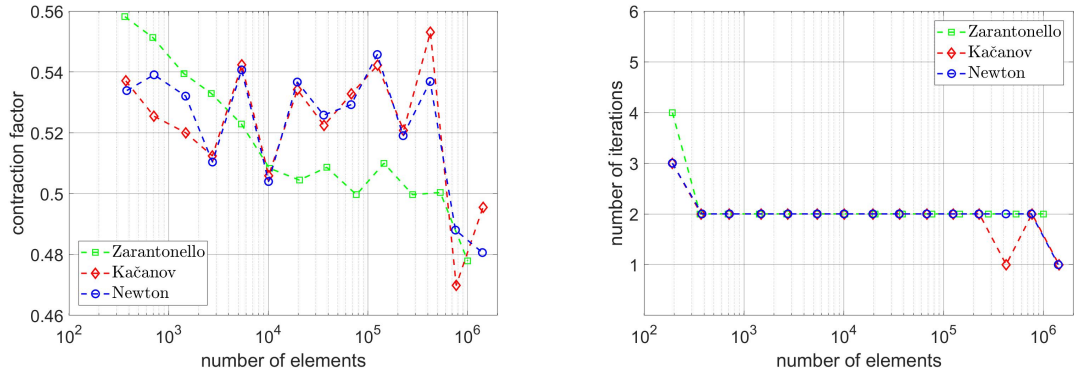


FIGURE 5. $\delta_Z = 0.3$ and $\lambda = 0.1$: The contraction factor \varkappa_N (left, see (24)) and the number of iterations (right) on each finite element space.

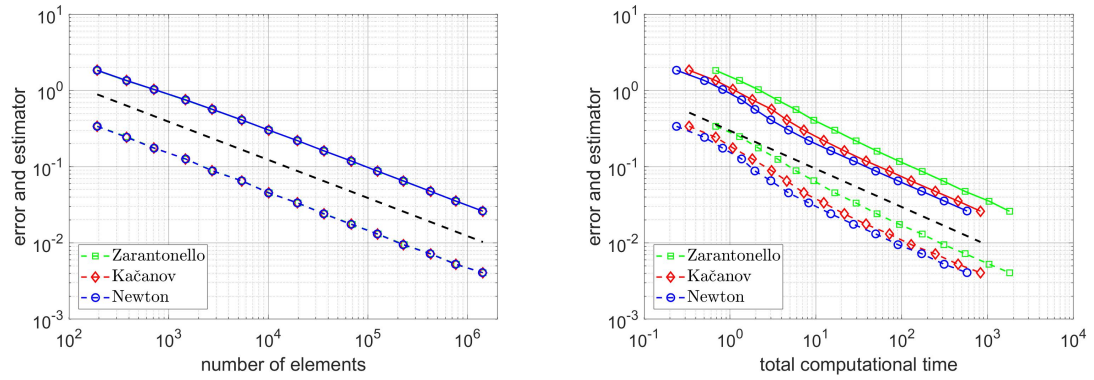


FIGURE 6. $\delta_Z = 0.3$ and $\lambda = 0.01$: Performance plot for adaptively refined meshes with respect to the number of elements (left) and the total computational time (right). The solid and dashed lines correspond to the estimator and the error, respectively. The dashed lines without any markers indicate the optimal convergence order of $-1/2$ for linear finite elements.

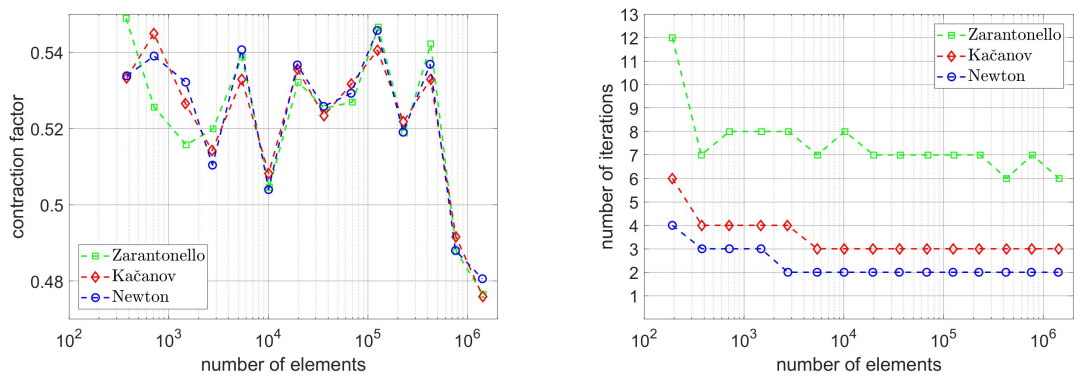


FIGURE 7. $\delta_Z = 0.3$ and $\lambda = 0.01$: The contraction factor \varkappa_N (left, see (24)) and the number of iterations (right) on each finite element space.

from [GHPS20]. In particular, the sequence generated by the adaptive iterative linearized finite element method (AILFEM, see Algorithm 1) converges linearly and, under some additional assumptions, even with optimal rate with respect to the overall computational cost. This is confirmed by our numerical test in the context of quasi-linear elliptic problems, where we also underline that the theoretical constraints on the adaptivity parameters $\lambda > 0$ and $0 < \theta \leq 1$ are less restrictive in practice.

REFERENCES

- [AW14] M. Amrein and T. P. Wihler, *An adaptive Newton-method based on a dynamical systems approach*, Commun. Nonlinear Sci. Numer. Simul. **19** (2014), no. 9, 2958–2973.
- [CFPP14] C. Carstensen, M. Feischl, M. Page, and D. Praetorius, *Axioms of adaptivity*, Comput. Math. Appl. **67** (2014), no. 6, 1195–1253.
- [CW17] S. Congreve and T. P. Wihler, *Iterative Galerkin discretizations for strongly monotone problems*, Journal of Computational and Applied Mathematics **311** (2017), 457–472.
- [FPW11] S. Funken, D. Praetorius, and P. Wissgott, *Efficient implementation of adaptive P1-FEM in Matlab*, Computational Methods in Applied Mathematics **11** (2011), no. 4, 460–490. MR 2875100
- [GHPS18] G. Gantner, A. Haberl, D. Praetorius, and B. Stifftner, *Rate optimal adaptive FEM with inexact solver for nonlinear operators*, IMA Journal of Numerical Analysis **38** (2018), no. 4, 1797–1831.
- [GHPS20] G. Gantner, A. Haberl, D. Praetorius, and S. Schimanko, *Rate optimality of adaptive finite element methods with respect to the overall computational costs*, Tech. Report 2003.10785, arxiv.org, 2020.
- [GMZ12] E. M. Garau, P. Morin, and C. Zuppa, *Quasi-optimal convergence rate of an AFEM for quasi-linear problems of monotone type*, Numer. Math. Theory Methods Appl. **5** (2012), no. 2, 131–156.
- [HW20a] P. Heid and T. P. Wihler, *Adaptive iterative linearization Galerkin methods for nonlinear problems*, Math. Comp. (2020), in press.
- [HW20b] P. Heid and T. P. Wihler, *On the convergence of adaptive iterative linearized Galerkin methods*, Calcolo (2020), in press.
- [Mit91] W. F. Mitchell, *Adaptive refinement for arbitrary finite-element spaces with hierarchical basis*, J. Comput. Appl. Math. **36** (1991), 65–78.
- [Neč86] J. Nečas, *Introduction to the theory of nonlinear elliptic equations*, John Wiley and Sons, 1986.
- [Zar60] E. H. Zarantonello, *Solving functional equations by contractive averaging*, Tech. Report 160, Mathematics Research Center, Madison, WI, 1960.
- [Zei90] E. Zeidler, *Nonlinear functional analysis and its applications. II/B*, Springer-Verlag, New York, 1990.